

from 12 to 40 m/s for the Japanese Geostationary Meteorological Satellite, but only 10 to 18 m/s for GOES winds. The greater disagreement between satellite and rawinsonde winds was largely due to height assignment error where there were strong vertical shears or differences in the times of observations. Low-level satellite winds differed by about 6 to 9 m/s from rawinsonde measurements.

### CO<sub>2</sub> Slicing Method

Data from 2 visible-infrared spin-scan radiometer atmospheric sounder (VAS) were utilized to determine simultaneous heights and velocities of cloud motion winds. A CO<sub>2</sub> cloud slicing technique was employed that combines the clear-air radiances with cloud radiances in the radiation transfer equation. The CO<sub>2</sub> slicing and absorption methods are presented here. Tracking of clouds can be accomplished by utilizing time sequences of CO<sub>2</sub> channel images as indicated by Menzel et al.<sup>5</sup> This CO<sub>2</sub> slicing method improves CMV determination. The cloud motions can be observed by the animation of channels 5, 8, and 10 in the infrared range of 6.7, 11.6, and 13.0  $\mu\text{m}$ .

The high resolution of wind measurement from satellite imagery detects atmospheric motion through measurement of cloud displacement. In a sequence of images from a geostationary satellite (GOES-7), clouds move with the wind, and from these images it is possible to describe the motions of the atmosphere.<sup>6</sup> Methods used to derive the "cloud drift" require using good geostationary satellite images of geometric fidelity with time intervals of 30 min between images. In order to get a greater density of cloud motion vectors close to the KSC station, they were selected manually. This was done by choosing a target, following it by eye, and letting the computer do the vectoring and pressure. This is the procedure used in assessing the CMV.

These results show a considerable improvement in the verification of the satellite winds over those reported by Whitney. There are several possible reasons for this improvement. First, the cloud motions were measured in a research mode where the pressures and time constraints of operational work do not apply. Second, the CO<sub>2</sub> method of determining the very important variable of cloud height is thought to be considerably more accurate than the old method of using the infrared window for obtaining heights. Third, the Jimsphere wind measurements used to verify the cloud motions have been shown to be more accurate than radiosonde wind measurements.<sup>7</sup>

The cumulative effects of these refinements in the procedure should naturally produce smaller errors than those found in previous verifications. However, the fact remains that a cloud motion is measured through the depth of the atmosphere in which the cloud exists, and never can be precisely compared with a balloon measurement at a particular level. Without knowledge of the cloud depth this difficulty cannot be overcome and will remain a source of error.

### Conclusion

This research has demonstrated the results of the comparison of measured winds between the FPS-16 Radar/Jimsphere Wind System and the GOES-7 Satellite. The scientific value of any satellite-sensed physical parameter such as wind must be validated by accurate in situ measurements. The in situ data were obtained by the Jimsphere balloon system, which has been used for the past three decades in measuring winds for the space shuttle launches. The Radar Wind Profiler plays an important role in monitoring winds for substantial profile changes during the day of launch. During the STS-37 and STS-43 Space Shuttle launches, the wind measurements were compared with NASA's 50-MHz Radar Wind Profiler. The results were a standard deviation of 1.66 m/s for the  $u$  component and 1.55 m/s for the  $v$  component, giving a standard deviation of 2.27 m/s for the vector wind. This role for the day of launch, when there are no clouds at all levels, is satisfied because the winds are light. These launch wind data of STS-37 and STS-43 at KSC, Florida, were compared with GOES-7 satellite wind data. The average distance of wind measurement between the GOES-7 satellite cloud winds and Jimsphere balloon winds was 65 km. The global comparison of satellite and Jimsphere vector winds shows a standard deviation of 3.15 m/s for STS-43 and 4.37 m/s for STS-37. The overall standard deviation of the vector wind was 3.76 m/s with a root-mean-square vector difference of 4.43 m/s. It was demonstrated that this unique comparison

of winds obtained by the Jimsphere and the Radar Wind Profiler provides a frame of reference for comparison with satellite data.

These results show a considerable improvement in the verification of the satellite winds over those previously reported. There are several possible reasons for this improvement. First, the cloud motions were measured in a research mode, where the pressures and time constraints of operational work do not apply. Second, the CO<sub>2</sub> method of determining the very important variable of cloud height is thought to be considerably more accurate than the old method of using the infrared window. Third, the Jimsphere wind measurements used to verify the cloud motions have been shown to be more accurate than radiosonde wind measurements.

The cumulative effects of these refinements in method should naturally produce smaller errors than those found in previous verifications. However, the fact remains that a cloud motion is measured through the depth of the atmosphere in which the cloud exists, and can never be precisely compared with a balloon measurement at a particular level. Without knowledge of the cloud depth, this factor cannot be allowed for and will remain a source of error.

### References

- <sup>1</sup>Susko, M., "Comparison of FPS-16 Radar/Jimsphere and NASA's 50 MHz Radar Wind Profiler," AIAA Paper 93-0758, Jan. 1993.
- <sup>2</sup>Smith, S., "Cross Spectral Analysis to Determine the Resolution and Precision of Jimsphere and Windsound Measurements," *Third International Conference on Aviation Weather System*, American Meteorological Society, Boston, MA, 1989, pp. 385-386.
- <sup>3</sup>Smith, E., and Phillips, D., "Measurements from Satellite Platforms," Annual Report on NAS5-11542, 1971-1972, Space Science and Engineering Center, Univ. of Wisconsin, pp. 1-53.
- <sup>4</sup>Herman, L. D., "The Current Stage of Development of a Method of Producing Cloud Motion Vectors at High Latitudes from NOAA Satellites," *Proceedings EUM P 10*, Washington, DC, 1991, ISBN 92-9110-0072, pp. 21-26.
- <sup>5</sup>Menzel, W. P., Smith, W. L., and Stewart, T. R., "Improved Cloud Motion Wind Vector and Altitude Using VAS," *Journal of Climate and Applied Meteorology*, Vol. 22, March 1983, pp. 377-384.
- <sup>6</sup>Whitney, L. F., Jr., "International Comparison of Satellite Winds—an Update," *Advances in Space Research*, Vol. 2, No. 6, 1982, pp. 73-77.
- <sup>7</sup>Anon., "Meteorological Data Estimates," Range Commanders Council/Meteorology Group, Document 353-387, White Sands Missile Range, NM, Sept. 1987.

H. R. Anderson  
Associate Editor

## Effect of Payload on Risk of Vehicle Loss Due to Engine Failure

Eric Queen\* and Alice Thompson†  
NASA Langley Research Center,  
Hampton, Virginia 23681

### Introduction

THE future of humanity's presence in space is critically dependent on cheaper, more reliable access to Earth orbit. One method to reduce costs while increasing reliability is to automate processes that have previously been performed by hand. Another method to increase reliability is to increase safety margins. However, this will result in a reduction of the amount of payload per

Received March 28, 1994; revision received Sept. 29, 1994; accepted for publication Nov. 19, 1994. Copyright © 1995 by the American Institute of Aeronautics and Astronautics, Inc. No copyright is asserted in the United States under Title 17, U.S. Code. The U.S. Government has a royalty-free license to exercise all rights under the copyright claimed herein for Governmental purposes. All other rights are reserved by the copyright owner.

\*Research Engineer, Vehicle Analysis Branch, Space Systems and Concepts Division. Member AIAA.

†Research Engineer, Systems Analysis Branch, Aeronautics Systems Analysis Division. Student Member AIAA.

launch. Both methods have merits, and any future launch system will incorporate both approaches. By using the proper combination of both of these ideas, cost and risk reductions may be realized that would be impossible using either idea alone. In the area of vehicle guidance, which has historically been performed prior to launch, great increases in performance can be achieved by implementation of an autonomous, on-board, real-time, optimal guidance scheme.<sup>1</sup> This paper discusses a preliminary investigation into the improvements available to a vehicle subject to engine failures that is capable of modifying its trajectory in-flight. This is compared with a similar vehicle for which an engine out at liftoff is assumed.

The National Launch System (NLS) was a series of unmanned heavy-lift launch vehicles proposed to be in operation by the turn of the century.<sup>2</sup> The largest vehicle of this series is considered in this report. This vehicle was to be a symmetric, 1.5-stage vehicle. By "1.5-stage" it is meant that engines are dropped at staging, but not tankage. At liftoff, the vehicle uses six identical main engines, four of which are booster engines discarded at staging. The two remaining engines are referred to as core engines. Each engine had vacuum thrust of 2595 kN. The "standard" case has a fixed staging 195 s after liftoff, which is the optimal staging time assuming a core engine out at liftoff. Staging of the boosters means a drop of 29,920 kg. In the cases addressed in this report it was assumed that the NLS burns all 765,433 kg of its available fuel to reach orbit. This means only the core (65,251 kg), shroud (4474 kg), and payload remain as orbit is reached. Under the assumption of an engine out at liftoff, the deliverable payload is approximately 17,000 kg. However, if all engines are working, or the engine that fails is a booster engine, it will be possible to get considerably more payload into orbit.

As the system matures, and confidence and reliability increase, the temptation to load the vehicle under the assumption of no engine failures will be great, since this would significantly reduce the price per pound of payload to orbit. The current work investigates the performance of an NLS vehicle that is laden beyond the engine-out-at-liftoff capability and that loses an engine at some later point in the trajectory. In this case, some orbit lower than the standard orbit may be adequate to prevent loss of the vehicle and payload. Here a minimum safe orbit is considered to be a circular orbit of  $148 \times 148$  km.

### Problem Statement

Two questions will be addressed in this work. Can the vehicle suffer an unexpected engine loss and still carry a full payload to an orbit high enough to avoid re-entry? And secondly, what is the relationship between payload mass and the ability of the vehicle to achieve orbit?

The first objective is to find the "best" possible orbit for a given engine-out time (EOT) with a fully loaded vehicle. Since no orbit with a perigee below 148 km will be considered acceptable, a final altitude of 148 km is imposed on the vehicle and the final velocity is maximized.

The problem is addressed using optimal-control theory, which leads to a two-point boundary-value problem. Since foreknowledge of the EOT will never be available, the nominal case for this study is defined by the case of all engines working with maximum payload. Note that this is different from the standard case, which assumes a core engine out at liftoff. For each EOT, then, the initial conditions are taken as the state of the nominal trajectory at the corresponding time. The minimum recoverable engine-out time (MREOT) is the minimum operation time for which the optimal final velocity is at least as great as the 148-km circular velocity for a given payload. This procedure is illustrated in Fig. 1.

The second objective is to determine the tradeoff between extra payload and engine reliability. For a smaller payload, the MREOT will be earlier in the ascent profile. The approach described above is repeated for a range of payload values until the MREOT reaches liftoff. The results of the study will be the identification of combinations of engine failure times with the corresponding payloads that achieve at least a minimum orbit.

### Solution Technique

The vehicle model used in this study is a point-mass NLS model with the angle of attack  $\alpha$  as the control variable. The four state

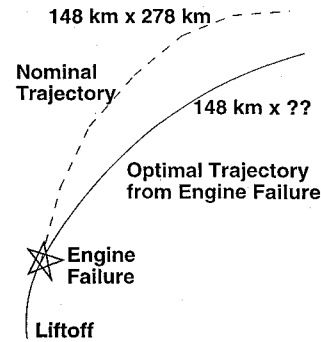


Fig. 1 Failure scenario.

variables in this model are as follows: vehicle mass, altitude, speed, and flight-path angle, denoted  $m$ ,  $h$ ,  $V$ , and  $\gamma$ , respectively. The equations of motion are

$$\dot{m} = \frac{-T_{\text{vac}}}{g I_{\text{sp}}} \quad (1)$$

$$\dot{h} = V \sin \gamma \quad (2)$$

$$\dot{V} = \frac{T \cos \alpha - D}{m} - \frac{\mu \sin \gamma}{(R_e + h)^2} \quad (3)$$

$$\dot{\gamma} = \frac{T \sin \alpha + L}{mV} + \left( \frac{V}{R_e + h} - \frac{\mu}{V(R_e + h)^2} \right) \cos \gamma \quad (4)$$

The vacuum thrust is  $T_{\text{vac}}$ , the net thrust is  $T$ , the specific impulse is  $I_{\text{sp}}$ , and the acceleration due to gravity at sea level is  $g$ . The earth's radius is  $R_e$ , and its gravitational constant is  $\mu$ . The drag and lift forces are denoted  $D$  and  $L$ , respectively, and are resolved from the normal and axial forces. The coefficients of the axial and normal forces were taken from wind-tunnel data. The net thrust is defined as

$$T = T_{\text{vac}} - A_e p \quad (5)$$

with  $A_e$  representing the total nozzle exit area. The atmospheric pressure  $p$  and density  $\rho$  were calculated using exponential models determined by a least-squares fit to selected values from the 1976 Standard Atmosphere.<sup>3</sup>

In order to limit the structural loads on the vehicle, a constraint is placed on the product of the dynamic pressure and the angle of attack,  $q\alpha$ . This product is not allowed to exceed 4267 Pa-rad.

Using the format of Bryson and Ho,<sup>4</sup> the performance index is

$$J = -V_f \quad (6)$$

with  $V_f$  being the final velocity. The initial boundary conditions are the initial mass, altitude, velocity, and flight-path angle at the time of engine failure and are obtained from the nominal trajectory. There is a step discontinuity in mass at staging, and the staging time is free to be determined to maximize the final velocity. The vehicle's final mass is initially constrained to be 94,796 kg. The MREOT is determined by varying the final mass until a minimum orbit can be reached. The final altitude is 148 km, and the final flight-path angle is zero.

### Results

It was assumed that all trajectories would follow the nominal until the time of an engine failure. A family of problems was posed as follows. First, the nominal trajectory and payload were determined. Then the state vector at various times along the nominal trajectory was used as the initial condition for problems with an engine failure and the same (nominal) payload. Finally, solutions were obtained for reduced payloads to determine the maximum payload corresponding to each time of engine failure. Multiengine failures were not considered. The problems were solved numerically using the Variational Trajectory Optimization Toolset (VTOTS).<sup>5</sup> The solutions were compared with the standard and nominal cases.

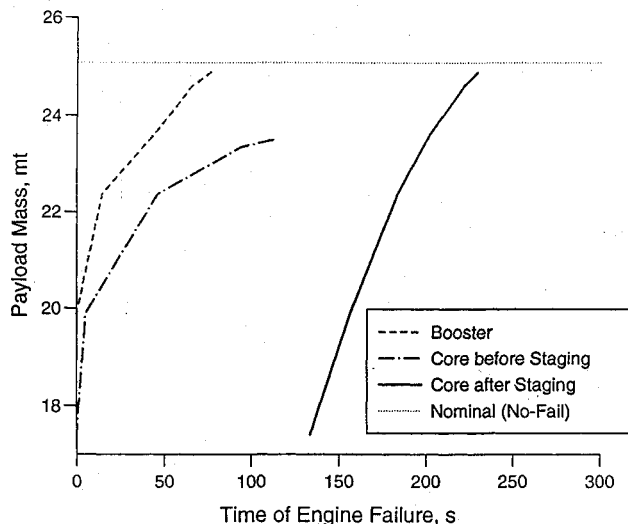


Fig. 2 Maximum payload to orbit vs time of engine failure.

In the nominal case, the vehicle reached the standard orbit of  $148 \times 278$  km carrying a 25,070-kg payload. The vehicle staged 134.3 s after liftoff. Orbit was achieved after 354.4 s.

To find the earliest failure time for which the vehicle could reach at least a minimum orbit, a series of problems were solved assuming loss of either a core or a booster engine at various points throughout the trajectory. For this series, the payload mass was fixed to that of the nominal. Initial conditions were taken from the nominal at 10- to 13-s intervals. It was seen that for a full payload, the vehicle could reach a minimum orbit if each booster operates at least 77 s after launch and only a booster failure occurs. Similarly, the MREOT for a core engine was 230 s, which is different for two reasons. Since there are only two core engines, loss of a core engine implies one-half thrust after staging. Also, the initial conditions were taken from the nominal case, which assumes no engine failures. The cases that involve engine failure after staging were constrained to have staged at the optimal staging time for the no-fail case. Since any booster failure necessarily occurs before staging, it was always possible in those cases to adjust the time of staging to increase the final velocity. However, for a core-engine failure before staging, the staging time could not be delayed long enough to meet acceptable final conditions with the nominal payload.

The process above was repeated for payloads that had been reduced by 1, 2, 5, 10, 20, and 30%. Figure 2 presents the maximum mass that can be carried to the minimum orbit as a function of time of failure of a booster or core engine. For payloads below 23,500 kg, there are two branches of the core-engine failure MREOT: one for failure prior to, and one subsequent to, staging. Again, this is due to the fact that if an engine fails prior to staging, the staging time can be shifted to compensate. After staging, that ability is lost. The 23,500 kg can be delivered to a minimum orbit if both core engines operate for 110 s of the first stage and no booster failure occurs, or if a core engine fails after 190 s and no booster failure occurs.

Note that loss of a core engine at staging yields the same results as loss of an engine at liftoff if the trajectory has been optimized assuming no engines are lost. In both of these cases, the vehicle would not reach minimum orbit. Also, initial loss of a core engine is more restrictive than initial loss of a booster engine by 2500 kg. The slopes of the curves in Fig. 2 are quite steep at the lowest payloads, so a willingness to accept the risk of an engine failure in the first few seconds might significantly increase the potential deliverable payload.

## Conclusions

A family of optimal-control problems for an NLS-type vehicle involving single engine failures has been solved. The solutions to these problems indicate that loading a vehicle under the assumption of a core engine out at launch may not be ideal. This study has partially quantified the added risk of additional payload by showing the maximum payload for various engine failure times. The ability to reoptimize trajectories midcourse in response to an engine loss coupled with a willingness to accept a degraded orbit, as an emergency measure, can result in much larger payloads for a given vehicle.

## References

- <sup>1</sup>Hardtla, J. W., Piehler, M. J., and Bradt, J. E., "Guidance Requirements for Future Launch Vehicles," AIAA Paper 87-2462, Aug. 1987.
- <sup>2</sup>Buchanan, H., "Overview of National Launch System with Emphasis on Cargo Transfer Vehicle," AIAA Paper 92-1387, March 1992.
- <sup>3</sup>Anon., *U.S. Standard Atmosphere*, 1976, U.S. Committee on Extension to the Standard Atmosphere, NOAA, NASA, USAF.
- <sup>4</sup>Bryson, A. E., Jr., and Ho, Y.-C., *Applied Optimal Control*, 1st ed., Hemisphere, Waltham, MA, 1975, pp. 42-89.
- <sup>5</sup>Bless, R. B., Queen, E. M., Cavanaugh, M. D., Wetzel, T. A., and Moeder, D. D., "Variational Trajectory Optimization Tool Set (VTOTS) Technical Description and Users Manual," NASA TM 4442, July 1993.

I. E. Vas  
Associate Editor